

Article

Evaluation of Different Chemical Mechanisms on O₃ and PM_{2.5} Predictions in Alberta, Canada

Mujtaba Shareef^{1,*}, Sunny Cho², David Lyder², Michael Zelensky¹ and Scott Heckbert¹¹ Alberta Energy Regulator, University of Calgary, Calgary, AB T2N 1N4, Canada² Alberta Environment and Parks, Edmonton, AB T5K 2J6, Canada

* Correspondence: mujtaba.shareef@aer.ca

Abstract: We evaluated the uncertainty associated with secondary pollutants formation due to different chemical mechanisms in photochemical modelling. The CMAQ modelling system was utilized in conjunction with CB6R3, SAPRC07, and RACM2 chemical mechanisms and compared the concentrations of various chemical species, including ozone (O₃) and particulate matter (PM_{2.5}). Using datasets from ambient monitoring stations, we assessed the performance of each of the mechanism in summer and winter. The concentrations of various chemical species predicted by the three mechanisms varied significantly. The differences are more evident in summer than in winter for most of the species, except for hydrogen peroxide (H₂O₂), methyl hydroperoxide (MEPX), and Secondary Organic Aerosol—Anthropogenic. We observed that the summer daytime O₃ predictions showed reasonable peaks at the three air quality monitoring sites, but the nighttime values under-predicted for all three mechanisms. In the winter, all three mechanisms tend to under-predict O₃. Differences in the mean O₃ values (bias) at the different sites, for the different seasons, are consistent with corrections made to previous modelling studies that modified KZMIN. PM_{2.5} predictions with RACM2 were slightly better. The dominant PM_{2.5} species in summer were sulfate and SOA-Bio, which may be attributed to non-mobile sources in the region, while NO₃ became dominant in winter due to more favorable conditions for forming this species, including lower temperatures and an elevated NH₄ to SO₄ ratio. We concluded that the differences in O₃ and PM_{2.5} predictions between the three mechanisms are significant, implying that when developing strategic and management actions are based on modelling, the most appropriate mechanism should be considered.

Keywords: CMAQ; chemical mechanisms; O₃; PM_{2.5}

Citation: Shareef, M.; Cho, S.; Lyder, D.; Zelensky, M.; Heckbert, S. Evaluation of Different Chemical Mechanisms on O₃ and PM_{2.5} Predictions in Alberta, Canada. *Appl. Sci.* **2022**, *12*, 8576. <https://doi.org/10.3390/app12178576>

Academic Editors: Tak W. Chan and Satoshi Irei

Received: 14 July 2022

Accepted: 21 August 2022

Published: 27 August 2022

Publisher's Note: MDPI stays neutral with regard to jurisdictional claims in published maps and institutional affiliations.



Copyright: © 2022 by the authors. Licensee MDPI, Basel, Switzerland. This article is an open access article distributed under the terms and conditions of the Creative Commons Attribution (CC BY) license (<https://creativecommons.org/licenses/by/4.0/>).

1. Introduction

Air pollution remain one of the most serious threats to human health and ecosystems, despite efforts to control anthropogenic emissions. Ground-level ozone (O₃) and particulate matter (PM_{2.5}) are two pollutants of most concern, given their adverse effect on human health and ecosystems [1–7]. However, O₃ and a significant portion of PM_{2.5} (secondary PM_{2.5}) are secondary pollutants formed by the complex synthesis of several precursor gases, such as volatile organic compounds (VOCs), oxides of nitrogen (NO_x), and sulfur dioxide (SO₂), in the atmosphere with an evolution and impact that may be difficult to predict [8]. Furthermore, given the limited availability of suitable temporal and spatial measurements of pollutants, atmospheric chemical transport models (ACTMs) are essential for estimating secondary pollutant concentrations. However, ACTMs are typically developed to understand place-based (urban/rural, high elevation) problems using updated chemical kinetics and photolytic rates, additional chemical species, and/or additional chemical pathways [9]. Furthermore, adjustments to the mechanical component of an ACTM, e.g., the minimum eddy diffusivity coefficient as a function of land use [10], if any, must be considered when evaluating an ACTMs performance. From an air-quality-management perspective, selection of the wrong ACTM may lead to incorrect conclusions regarding

the influence of precursors on the formation of secondary pollutants and, subsequently, a poor management response. Changes to the vertical diffusivity, mixing height, etc., [11] may also introduce an ad hoc bias in the model, which may be difficult to interpret. Hence, combining suitable temporal and spatial monitoring data, when available, serves to both guide in the selection of the most appropriate ACTM as well as better inform the choice of effective mitigation strategies.

Many chemical mechanisms have been developed for ACTMs to address the issues associated with urban/rural O₃ formation. Three of the most widely used mechanisms are the Regional Atmospheric Chemistry Mechanism 2 (RACM2) model [12], the State Air Pollution Research Center (SAPRC07) model [13], and the Carbon Bond 6 (CB6) model [14–16].

The RACM2 model is built on earlier ACTMs, in particular the Regional Acid Deposition Model (RADM) [17] and its extension (RADM2) [18], which had been developed to understand the formation of atmospheric acids, the formation of organic and inorganic peroxides, and aqueous chemistry involving the oxidation of SO₂ in urban/polluted and rural/less polluted areas, respectively. Improved reaction rates, updated reaction schemes and product yields for a more extensive suite of inorganic and organic compounds continued with the development of the RACM [19] and RACM2 [12]. Of note were improvements to explicitly include organic compounds, i.e., alkanes, alkenes, carbonyls, and aromatics, believed to be significant reactants in a relatively clean (low NO_x) atmosphere. While expanding the chemistry consideration of computational constraints was made by lumping species of similar reactivity together, the version of RACM2 [20] employed here comprised 54 explicit species and 80 lumped species, making available 582 reactions in total.

SAPRC07 [21] is likely the most comprehensive and adaptable photochemical model considered here, allowing for specific representation of up to 780 types of VOCs [13], when needed for particular reactivity assessments of O₃ formation. However, for computational purposes, it also makes use of a lumped-chemical model developed from the earlier SAPRC99 [22], which uses a numerical parameter to weight the contribution from individual reactions. Additional improvements to the model included updated rate constants, updated photolysis rates, updated chlorine chemistry involving aldehydes and ketones, and, perhaps most importantly for this discussion, improved treatment of peroxy radicals under low NO_x conditions leading to better estimates of the formation of hydroperoxides and Secondary Organic Aerosols. The version of SAPRC07 (saprc07_ae6_aq) employed in this work comprised 97 explicit species and 64 lumped species, which allowed the modelling of 732 reactions.

The CB model was originally developed in the 1970s [16], with the most commonly used version being the CB-IV model [14]. The CB models use a blend of explicit species (e.g., ethene, isoprene, formaldehyde) with the remaining organic species represented by a lumped-structure model made up of a simple sum of the more basic carbon bond types making up the species. In some cases, the implied reactivity may be moderated by assigning some of the carbon atoms to a non-reactive group. The lumped-structure approach allows the simple addition of new organic species but may make interpretation of the predicted concentrations complicated. Significant changes were incorporated into the CB05 model [15] including updated kinetic reaction and photolysis rates, additional inorganic pathways, and improved organic chemistry related to alkanes, alkenes (particularly isoprene), and oxygenated products and intermediaries [23]. Alkyl nitrates in the model are more reactive, liberating more NO₂, while simultaneously allowing for greater deposition of the soluble alkyl nitrates. The net results of these improvements in CB05 are the higher predicted concentrations of O₃ during the summer and winter compared to CB-IV. The current CB version is CB6R3 [24], which was developed from CB6R2 to better represent wintertime high-ozone events in the Rocky Mountains, where modelled O₃ was significantly lower (~one third) than the observed O₃, by accounting for temperature and pressure effects on alkyl nitrate formation not accounted for in earlier CB models [25]. In particular, the reduced rate of formation of alkyl nitrates at lower temperatures enhanced the formation of O₃, given the additional availability of nitric oxide (NO) and alkanes to

produce O₃. The prediction of O₃ did improve using CB6R3, albeit modestly, but elevated NO_x (total nitrogen containing species—NO_x) species, particularly nitric acid, in both summer and winter, suggests additional research on reaction rates and/or removal processes is warranted [26]. For this work, we used cb6r3_ae6_aq, which comprised 60 explicit species and 68 lumped species, allowing the modelling of 339 possible reactions.

The three chemical mechanisms discussed above all share the concept of reaction rates and products; however, as previously stated, they differ in terms of rate constants, photolysis (due to pressure and temperature changes), and the treatment of organic and inorganic chemistry. Several studies [9,27–33] have compared these mechanisms and found considerable variations in the model predictions, particularly for O₃. Kitayama et al. [34] investigated uncertainties in O₃ formation caused by SAPRC07, CB05, RADM2, and SAPR99 and found that differences in reaction rate constants and lumped volatile organic compounds may be the cause of the differences in O₃ production. Chen et al. [35] compared the RADM series of ACTMs to the RACM series and noted the greatest daily maximum O₃ values predicted for RACM2 used updated photolysis rates, particularly more accurately predicted HCHO and NO₂ photolysis rates, which led to enhanced OH radical production. Cao et al. [36] compared the CB6 series (CB6r1, r2, r3) under urban conditions and noted the sensitivity of these models to temperature and reduced O₃ production, due to the enhanced formation of organic nitrates. To the best of our knowledge, all of these studies used the default value for KZMIN, so they did not consider the impact on O₃ formation due to the variation in KZMIN employed in this paper.

Alberta is Canada's largest oil-producing province and the heart of the country's oil and gas industry. Greenview Municipal District (MDGV) is in northwest Alberta and is well-known for its oil and gas rich geology. In 2019, the MDGV area had 391 wells and produced 3.6 million m³ of oil and 37.3 billion m³ of natural gas. There has been considerable growth in the area, with an increase of 64.0% production of natural gas over the previous five years [37]. Due to the region's extensive development of the oil and gas industry, the regional ambient air quality, particularly NO₂, O₃, and PM_{2.5}, is of concern. The Canadian Council of Ministers of the Environment [38] recommends that air quality be managed through an air zone management framework (AZMF). As shown in Table S1, AZMF categorizes stations based on pollutant concentrations and assigns a suitable color to each one. An examination of historical monitoring station data in this area (Figures S1–S3) reveals that some stations require active air quality management, as defined by Canadian Ambient Air Quality Standards or CAAQS [38]. Given the possible variation in modelling results attributable to differences in chemical mechanisms, sensitivity to photolysis rates and temperature, and the interplay between organic and inorganic chemistry, it is important to select the correct model that involves the relevant precursors, in order to properly assess policy options when developing mitigation scenarios to meet federal and provincial O₃ and PM_{2.5} standards. This discussion must also be made in the context of any variation in the bias for O₃ formation attributable to the choice of KZMIN.

This paper examines the differences in predictions of O₃, some gas-phase O₃ precursors, and PM_{2.5} between three chemical mechanisms, CB6R3, SAPRC07, and RACM2, as implemented in the Community Multi-Scale Air Quality (CMAQ) model [29]. The predictions are evaluated against monitoring station data for different locations in the MDGV as well as relative variation in O₃ and PM_{2.5} predictions across the region during the summer and winter months. The primary goal is to identify a chemical mechanism that can be used to model secondary pollutants in the MDGV region and potentially be applied more broadly to Alberta, which also takes into consideration the impact of variation in the model's vertical diffusivity due to land use.

2. Materials and Methods

2.1. Study Area and Models

The study area encompasses the MDGV and approximately 20 km beyond its boundary (Figure 1). Receptors were placed on a 4 km grid spacing that matches the meteorolog-

ical grid. Meteorology-Chemistry Interface Processor (MCIP 4.4) uses output files from Weather Research and Forecasting (WRF; [39]) meteorological model (Version 3.9.1.1) to generate meteorological data, which are used by both emissions and chemistry models. The meteorology used in this study was obtained from the Alberta provincial air quality photochemical modelling study [10]. Emissions modelling utilized the Sparse Matrix Operator Kernel Emissions (SMOKE 4.8.1) modelling system.

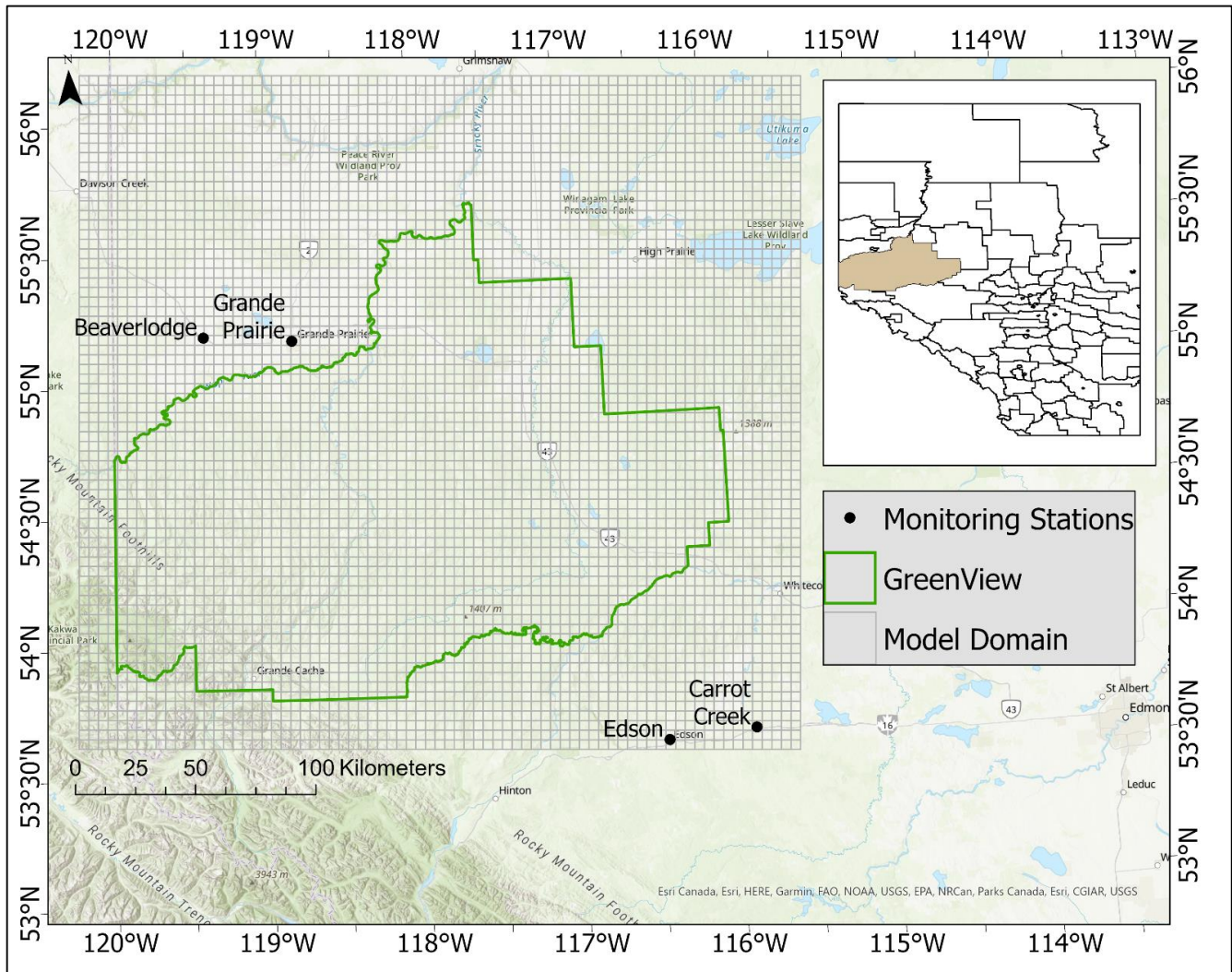


Figure 1. Study area showing model domain, grids, and monitoring stations.

SMOKE modelling provides the initial spatial and temporal allocation of emission inputs, as well as any chemical speciation required for each hour. The emissions inputs were generated for three mechanisms (CB6R3, SAPRC07, and RACM2). Simulations with different chemical mechanisms were performed using the Community Multiscale Air Quality (CMAQ 5.3.2) model, which is a 3D grid-based air quality model developed and maintained by Community Modeling and Analysis System. CMAQ simulates the formation of ozone, photochemical oxidants, and secondary particulate matter and the deposition of pollutants such as acids, toxic pollutants, and nitrogen species. It is an active open-source project that continuously enhances the accuracy and efficiency of photochemical modelling, by taking advantage of state-of-the-art multi-processor computing techniques. Table 1 summarizes the CMAQ model configurations used for all simulations in this study. The initial and boundary conditions were obtained from the Alberta provincial air quality photochemical modelling study [10]. The simulations were conducted for one month in summer (July 2013) and one month in winter (December 2013).

Table 1. CMAQ model 5.3.2 configuration.

Model Option	Configuration
Horizontal Grid Mesh	4 km
Vertical Grid Mesh	22 layers up to 100 mb
Gas-Phase Chemistry	CB6R3, SAPRC07 and RACM2
Aerosol Chemistry	AE6
Secondary Organic Aerosols	SORGAM
Meteorological Processor	MCIP Version 4.4
Horizontal Transport	PPM
Horizontal Diffusion	K-theory spatially varying
Vertical Advection Scheme	Yamartino
Vertical Eddy Diffusivity Scheme	ACM2
Diffusivity Lower Limit	Kzmin = 0.01 to 2.0 m ² /s (PURB option) (KZMIN set to true)
Deposition Scheme	M3dry
Land Surface Model (LSM)	Noah

2.2. Monitoring Stations

Four continuous air quality monitoring stations (one urban, two industrial, and one rural) within the study area/modelling domain are shown in Figure 1. Grande Prairie station is located near the urban area of the same name and is dominated by urban activities; hence, it is considered an urban station. There is considerable industrial activity in the vicinity of Beaverlodge and Carrot Creek. These two stations are considered industrial stations. Edson is predominantly surrounded by rural landscapes. These monitoring station datasets were used to assess model performance.

2.3. Emissions

In this study, the 2013 Alberta emission database was used, which was developed by harmonizing several emission sources from regional, provincial, and national levels [40–42]. The data sources and development methodology are described elsewhere [10]. Table 2 presents emissions breakdowns based on points and area sources as well as based on the oil and gas sector for each pollutant. The biogenic model, MEGAN 2.1 (Model of Emissions of Gases and Aerosols from Nature), was applied using daily meteorology from the WRF model to generate daily emissions. Land cover variables such as emission factors, leaf area index, and plant functional types were taken from the biospheric atmospheric interactions group at the University of California Irvine [43].

Table 2. 2013 Annual point and area emission sources of primary pollutants in the modelling domain.

Type	Emissions (tonnes)						
	SO ₂	NO _x	VOCs	PM ₁₀	PM _{2.5}	CO	NH ₃
Point Sources Oil and Gas Extraction	15,437	57,712	31,605	799	739	55,391	17
Point Sources Other than Oil and Gas Extraction	1794	6051	2040	1173	811	9789	67
Area Sources (biogenic, on-road, off-road, residential/commercial, industrial (not large stacks), waste management, road, fugitive, construction dust)	315	39,058	22,466	146,828	45,706	79,994	9651
Total	17,546	102,821	56,111	148,800	47,256	145,174	9735

In the modelling domain, total SO₂, NO_x, and VOCs emissions in 2013 were approximately 17.5 kt, 102 kt, and 56.1 kt, respectively. The major contributors to SO₂ and NO_x emissions are oil and gas point sources, while primary PM₁₀ and PM_{2.5} emissions are released predominantly from area sources. Since the model is run for emissions in July and December, spatial distribution of various pollutants in these months are presented in Figure 2. The emissions are observed to be high near Grande Prairie and Beaverlodge in the north and Edson in the south. Dense concentrations are also observed towards northwest and southeast of the domain likely due to the boundary conditions, i.e., the terrain is becoming significantly elevated towards the southwest. NO_x and PM_{2.5} are slightly higher in July, while VOCs are higher in December (Figure 2).

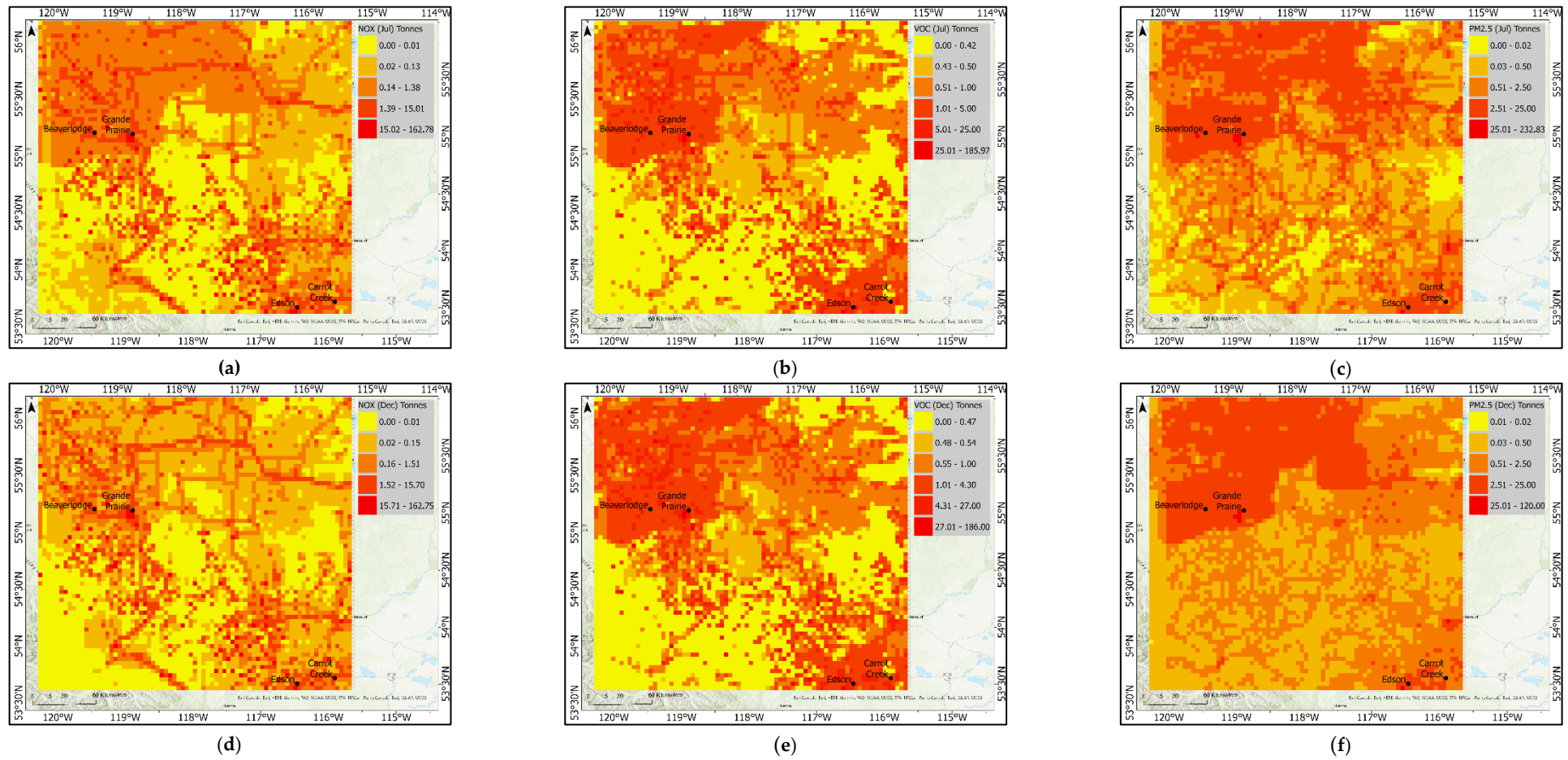


Figure 2. 2013 Spatial distribution of NO_x, VOC, and PM_{2.5} emissions in July (top) and December (bottom) in the modelling domain. (a) NO_x (summer), (b) VOC (summer), (c) PM_{2.5} (summer), (d) NO_x (winter), (e) VOC (winter), (f) PM_{2.5} (winter).

2.4. Model Performance Evaluation

The modelled concentrations are paired with data from air quality monitoring stations over time and compared against a performance benchmark (Table 3) for three mechanisms. The model results are compared to a set of numerical “goals” and less restrictive “criteria” performance benchmarks. Emery et al. [44] recommended the use of Normalized Mean Bias (NMB) and Normalized Mean Error (NME). Another set of benchmarks that are widely used was established by the U.S. Regional Planning Organizations (RPOs) based on Fractional Bias (FB) and Error (FE) [45]. Each of these metrics may be subject to particular limitations, e.g., some are unbound in their positive value, but collectively they will provide a weight of evidence estimate of model performance.

Table 3. Definitions of statistical model performance evaluation measures and performance benchmarks.

Statistical Measure	Mathematical Expression	Performance Benchmark Goals	Criteria
Normalized Mean Bias (NMB) (%)	$\frac{\sum_{i=1}^N (P_i - O_i)}{\sum_{i=1}^N O_i} \times 100$	MDA8 O ₃ < ±5% 24 h PM _{2.5} < ±10%	MDA8 O ₃ < ±15% 24 h PM _{2.5} < ±30%
Normalized Mean Error (NME) (%)	$\frac{\sum_{i=1}^N P_i - O_i }{\sum_{i=1}^N O_i} \times 100$	MDA8 O ₃ < 15% 24 h PM _{2.5} < 35%	MDA8 O ₃ < ±25% 24 h PM _{2.5} < ±50%
Fractionalized Bias (FB) (%)	$\frac{2}{N} \sum_{i=1}^N \left(\frac{P_i - O_i}{P_i + O_i} \right) \times 100$	24 h PM _{2.5} < ±30%	24 h PM _{2.5} < ±60%
Fractional Error (FE) (%)	$\frac{2}{N} \sum_{i=1}^N \left \frac{P_i - O_i}{P_i + O_i} \right \times 100$	24 h PM _{2.5} < 50%	24 h PM _{2.5} < 75%

MDA8—Maximum Daily 8 h Average

3. Results and Discussion

3.1. Precursors

The impact of three mechanisms, i.e., CB6R3, SAPRC07, and RACM2, on study-area mean concentrations of hydroxyl radical (OH), hydrogen peroxide (H₂O₂), methyl hydroperoxide (MEPX), peroxyacetyl nitrate (PAN), total nitrate (TNO₃), and oxides of nitrogen (NO_x) is analysed and discussed below. These species are precursors to the formation of O₃ and PM_{2.5}. The summer and winter monthly mean predicted concentrations by the three mechanisms and the percentage differences are summarized in Figure 3.

3.1.1. OH

The atmospheric oxidation capacity is determined by the presence of OH, as it reacts with many trace species in the atmosphere. With respect to CB6R3, both SAPRC07 and RACM2 produced elevated O₃ levels in the summer (SAPRC07 ~30% increase, RACM2 ~100% increase), as shown in Figure 3a. Winter concentrations of OH preserved the same ordinal ranking as summer, albeit the O₃ levels were significantly lower than summer. Differences between the winter O₃ levels for the three models are probably not significant. Some of the reasons that can be attributed to this high OH production by RACM2 are as follows. Firstly, RACM2 produces more O₃ and, subsequently, generates more O atoms under photolysis, with the O atoms reacting with H₂O to produce OH radicals. Secondly, the lower reaction rate of NO₂ + OH in RACM2 consumes fewer OH radicals from the atmosphere compared to CB6R3 and SAPRC07, as suggested by similar comparative studies between CB05TU and SAPRC07 [9,32]. Modelling studies comparing CB6R3 to CB05TU in the continental U.S. show an increase in the OH produced of ~25% for CB6R3 [23], which should reduce the OH deficit in the CB models; but, nevertheless, under the conditions considered (temperature, humidity), CB6R3 produced the least OH.

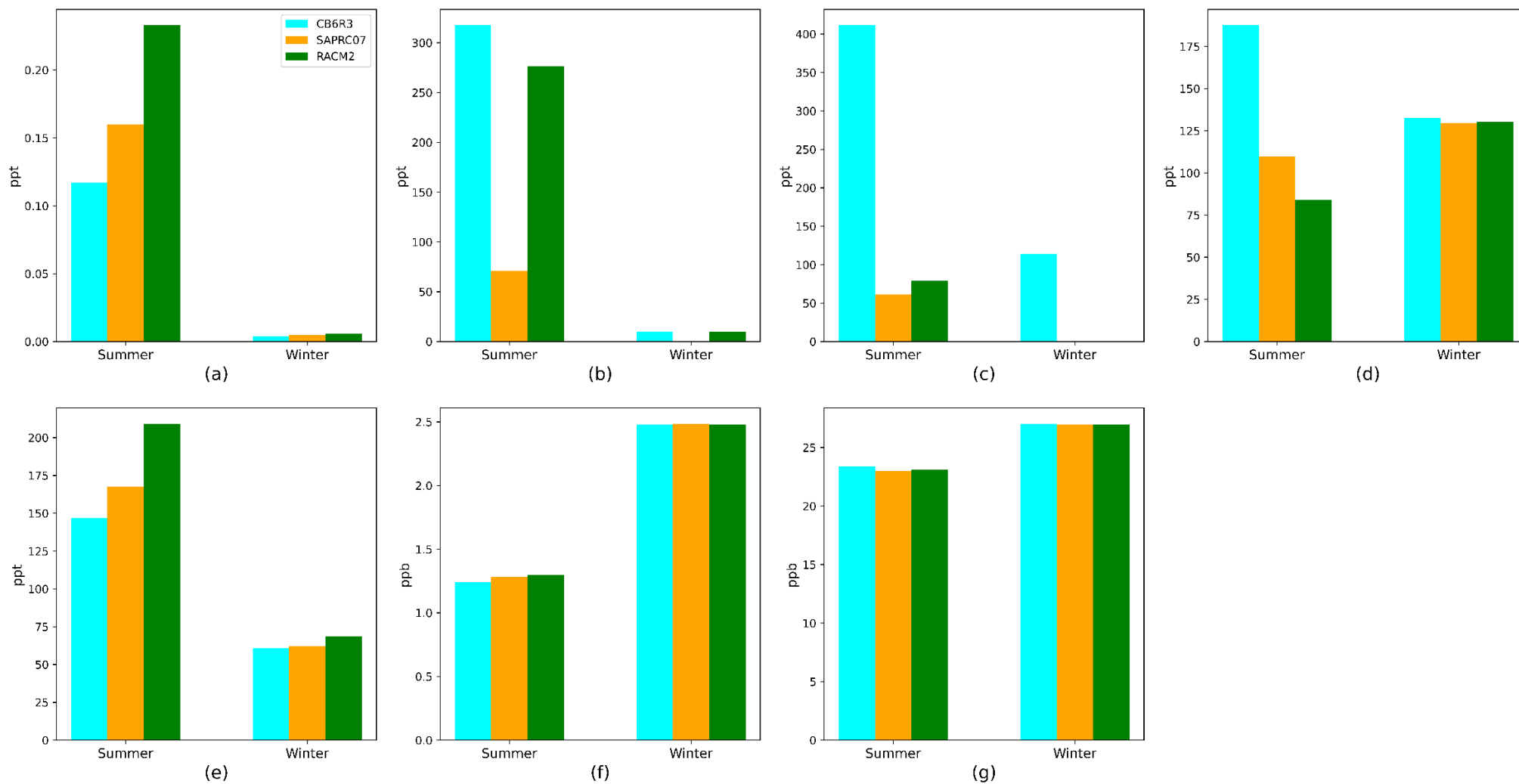


Figure 3. Comparison of CB6R3, SAPRC07, and RACM2 predicted monthly mean values for (a) OH, (b) H₂O₂ (SAPRC07 value in Dec is very small when compared to CB6R3 and RACM2) (c) MEPX (SAPRC07 and RACM2 values in Dec are very small when compared to CB6R3), (d) PAN, (e) TNO₃, (f) NO_x, (g) O₃.

3.1.2. H₂O₂

H₂O₂ exists in substantial amounts in both gaseous and aqueous phases inside clouds, and it is considered the most efficient oxidant in the aqueous phase [46]. In both summer and winter, CB6R3 and RACM2 produced significantly higher H₂O₂ than SAPRC07 as shown in Figure 3b. Summer H₂O₂ levels are generally greater than in the winter for all three mechanisms. The formation of H₂O₂ in CB6R3 and SAPRC07 is similar, except for the additional reaction OH + OH = H₂O₂ in CB6R3. However, it also has an additional destruction reaction (H₂O₂ + O = OH + HO₂). RACM2 produced additional H₂O₂ because of the reactions of O₃ with different organic compounds (such as alkenes). This supports the findings of Sarwar et al. [32], while in the study of Shareef et al. [9], RACM2 produced the highest H₂O₂ due to the arid atmospheric conditions of the area where the model was simulated.

3.1.3. MEPX

The reaction of the methyl peroxy radical or bicarbonate with HO₂ produces MEPX, while it is destroyed by photolysis and the reaction with the OH radical. The season results for MPEX are shown in Figure 3c. CB6R3 is the only mechanism that explicitly includes both formation pathways, with RACM2 and SAPRC07 only able to produce ~47% of the MEPX from the HO₂ pathway alone compared to the MEPX produced by CB6R3. The destruction of the MEPX in the CB6R3 mechanism is also greater than RACM2 and SAPRC07. The lower destruction rate of RACM2 compensates for, to a large extent, its lower formation rate relative to the CB6R3 mechanism. The lower destruction rate in SAPRC07 does not compensate as much, so its production is expected to be lower on this basis alone. However, clearly in this study the bicarbonate pathway for the formation of MEPX in CB6R3 is a key contributor. It is certainly contributing to the additional MEPX predicted in the summer, allowing for the variation in OH and photolysis rates, while it is the dominant formation mechanism in the winter when there is no OH available and the light levels are low.

3.1.4. PAN

PAN is one of the components of photochemical smog and forms from a sequence of reactions where aldehydes, ketones, and other oxygenated VOCs combine with OH to form an acetyl radical, which then combines with NO₂ to form PAN [47]. PAN formation in the three mechanisms are similar, though CB6R3 lumps acetyl nitrate output into two categories (PAN, PANX), while RACM2 uses four (PAN, PPN, MPAN, OPAN) as does SAPRC07 (PAN, PAN2, PBZN, MAPAN), depending on the precursor oxygenated VOCs. The formation rate for PAN from the acetyl radical in RACM2 is 8% less than the other two [48,49]. PAN may be destroyed by the reversal of the same PAN-forming mechanism back to the acetyl radical as part of a cycle as well as by its interaction with OH. The cycling between PAN and its acetyl radical precursor is faster in the summer than the winter. The speed of removal of PAN via the OH channel is slow in the summer and depends on the species of the acetyl radical present in the winter. The acetyl radical may also be destroyed via interaction with NO, HO₂, and RO₂, which is fast limiting the formation of PAN [47]. Finally, RACM2 has an additional photolytic reaction removing PAN from the cycle. The net result is more varied production of PAN amongst the three mechanisms in the summer, due to the speed of formation (and destruction), the lumping process, and the additional removal of PAN in the RACM2 mechanism. The winter production of PAN is less varied as it is slower, there is less variability in the composition of the alkyl radicals due to the reduction in biogenic emissions, and the light levels are low. During summer, CB6R3 produced about 55% and 60% more PAN than SAPRC07 and RACM2, respectively. There were no significant differences between the mechanisms in winter.

3.1.5. TNO₃

Modelling total nitrate TNO₃ (=NO₃ + HNO₃(g)) is complex, given the interplay that occurs between particulate NO₃ radical and HNO₃(g). This interplay must consider the partition between the particulate phase and gas phase of these different species that depend

on temperature, relative humidity, and surface chemistry [50]. HNO_3 is primarily formed by the oxidation of NO_2 by OH during daytime. At night, NO_2 is titrated by O_3 to form NO_3 plus O_2 , with the NO_3 further combining with NO_2 to form the reservoir species, N_2O_5 . In the presence of gaseous water, N_2O_5 will form HNO_3 , but this last reaction is highly variable, favoring the formation of HNO_3 when the temperature is low and the relative humidity is high. RACM2 produced approximately 45% and 21% more TNO_3 than CB6R3 and SAPRC07, respectively, in the summer. This ordering followed the same pattern as in the winter, but variation between the mechanisms was only a few percentage points, with the mean absolute values $\sim 30\%$ of the RACM2 summer value, as shown in Figure 3e. CB6R3 has the highest equilibrium rate followed by that SAPRC07 (93% of CB6R3's rate) and RACM2 (88% of CB6R3's rate), but RACM2, and to a lesser extent SAPRC07, produced more OH than CB6R3, which should result in higher HNO_3 and, hence, TNO_3 production. This pattern was seen elsewhere in a similar comparative study using CB05TU [31], but it has been noted that TNO_3 production has increased by $\sim 16\%$ in CB6R3 [23].

3.1.6. NO_x

NO_x plays an important role in the formation of O_3 . RACM2 produced about 5% higher concentration than CB6R3 and SAPRC07 mechanisms in July, as shown in Figure 3f. In December, the concentrations increased by two-fold, and there were no significant differences in the mechanisms. The SAPRC07 and RACM2 have more NO/NO_2 sink terms than CB6R3, and the reaction rates are much lower. High wintertime NO_x is a general phenomenon in the region and is also observed by [10].

3.2. O_3

3.2.1. Diurnal Variation

Since O_3 is a photochemical pollutant, its diurnal variation is important to understand. Figure 4 illustrates the diurnal plot for the Edson, Grande Prairie, and Beaverlodge air monitoring stations. The station diurnal plots include O_3 collected at the respective stations in addition to the predictions by the three mechanisms. The diurnal variation of O_3 follows a standard pattern over the course of the day by increasing after sunrise, reaching a maximum at noontime, and subsiding towards the evening. The pattern is more prominent in the summer than in the winter, as O_3 production is elevated due to higher temperatures and actinic flux [51]. All three mechanisms share many of the same pathways and reaction rates for the inorganic formation and destruction of O_3 . The organic pathways for the formation and destruction of O_3 are more complicated to understand, given the differences in definition or clumping of the organic compounds involved, but the similarity of the predicted O_3 levels suggests the organization of the organic compounds is essentially the same. In addition, the reaction rates for the formation via the many available organic pathways are lower, in general, than the inorganic pathways. One notable exception to this is the formation of O_3 from some ketones with the hydroxyl and peroxide ions in the CB6R3 model, which shows an elevated O_3 formation rate that is comparable to the inorganic pathways.

There are two qualitative comparisons we can make between the different mechanisms and O_3 observations that may shed light on the quality of the mechanisms: the first is the general fit by the mechanisms to the diurnal O_3 pattern, and the second is the hourly dispersion of O_3 values within each mechanism and within the observations.

In general, during the summer, all three mechanisms produce reasonable peak values of O_3 at all three sites. However, the nighttime values as well as the dawn and dusk values of predicted O_3 for all three mechanisms are generally lower than observations. One notable exception is at the Edson site, where the predicted dawn values are higher than observed. In the winter, all three mechanisms tend to under-predict O_3 , though there is some variability in the degree of this from site to site and for the time when it occurs. In a previous study undertaken in Alberta [10], it was noted that the variation in KZMIN (Table 1: KZMIN = $0.1 \text{ m}^2/\text{s}$ urban, $2.0 \text{ m}^2/\text{s}$ rural) allowed better fitting of mean predicted primary species and O_3 concentrations to observations. Too high of a

KZMIN resulted in an over-prediction of O₃ at night, and too low of a KZMIN resulted in an over-prediction of the primary species. The selected KZMIN values may not represent the optimal values for diffusion in the Planetary Boundary Level (PBL) and may account for some of the discrepancy between the predicted and observed O₃ values. Additional local effects, i.e., winter pile burning or wood heating, may account for some of the intermittent variability seen during the winter [10].

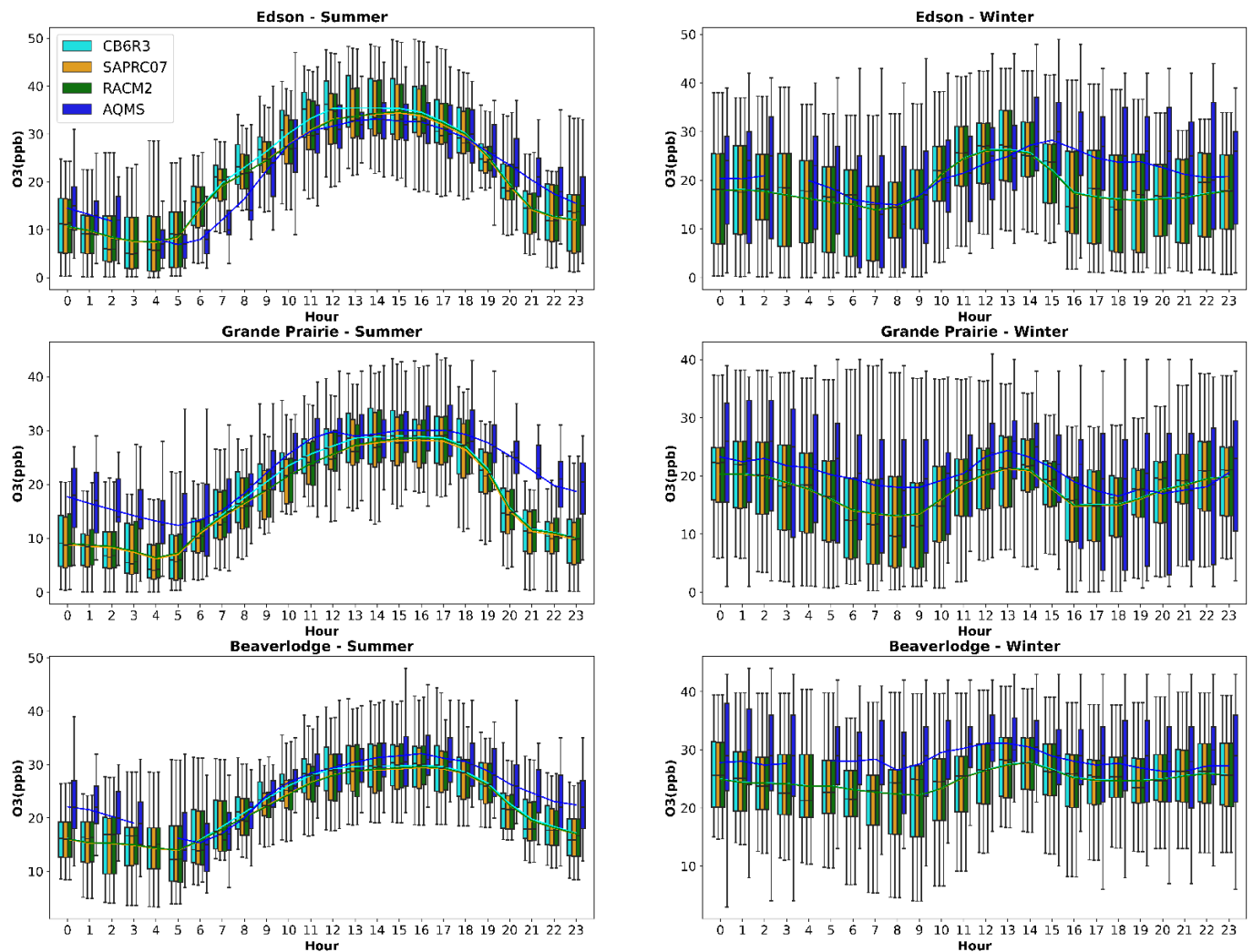


Figure 4. Diurnal variation of O₃ between three chemical mechanisms and ambient monitoring data at three monitoring stations in summer (left panel) and winter (right panel).

The dispersion of predicted hourly values may provide some insight into the performance of the different mechanisms. In all cases, it should be noted that the hourly variability for the three mechanisms is similar. This is not surprising, given the common photochemical reactions and rates the mechanisms are built on. During the summer, the night, dusk, and dawn variability in the mechanisms and the observations are similar. During daytime, there is less variability in the predicted O₃ values than the observed values, which may indicate there are some additional pathways for the creation or destruction of O₃. Perhaps the added ketone pathways included in the CB6R3 mechanism are pointing at the need to further identify and include similar pathways, or perhaps the reaction rates are not quite right.

Overall, all three mechanisms do a reasonable job of modelling the time series of O₃ at the three sites considered. From an air-quality-management perspective, it is important to understand the impact of changing the dispersion properties of the PBL, i.e., the effect

of KZMIN, as well as understanding some of the limitations in the responsiveness of the different mechanisms due to the pathways included. The CB6R3 mechanism shows a very slight elevation in O_3 (Figure 3g) that suggests the need for some additional organic pathways and some modifications in the existing pathways to better capture the diurnal evolution of O_3 , even allowing for the variation attributable to KZMIN.

3.2.2. Spatial Variation of O_3

The spatial variation of mean hourly O_3 predicted by CB6R3 in summer and winter, as well as the corresponding differences with SAPRC07 and RACM2, are shown in Figure 5. O_3 levels are generally observed as high near the modelling domain's boundaries, particularly in the southwest and east of the domain. Elevated O_3 levels towards the southwest could be in part due to increased elevation in this direction as well as reduced NO_x and VOC emissions, which would effectively remove O_3 . A similar enhancement in O_3 levels is seen in the east, where NO_x and VOC emissions are reduced. Moreover, higher concentrations are predicted at the Beaverlodge and Edson stations, while relatively lower concentrations are predicted at Grande Prairie. O_3 predictions (Figure 5) and the corresponding comparison with emissions (Figure 2) in the summer and winter months are discussed below.

Summer

When the CB6R3 case was compared to the SAPRC07 and RACM2 cases, both SAPRC07 and RACM2 produced 1%–3% less O_3 in low NO_x and low VOC areas (the most-eastern selected region is shown in Figure 2a). In high NO_x and VOCs areas such as Grande Prairie (the most-western selected region), SAPRC07 and RACM2 produced up to 6% less O_3 than CB6R3, as observed in Figure 5b,c. CB6R3 does seem to be the better performer in this region (Grande Prairie, Beaverlodge), as seen in Figure 6. In regions of low NO_x /moderate VOCs (the second-most-western selected region), there is a similar but reduced discrepancy in predicted O_3 by both SAPRC07 and RACM2 relative to CB6R3, while regions with moderate NO_x /low VOCs (continuing eastward to the next selected region) show a greater reduction in this discrepancy. This implies that CB6R3 produces higher levels of O_3 in the presence of higher VOCs and NO_x levels, relative to the SAPRC07 and RACM2 mechanisms, while producing similar levels of O_3 amongst all mechanisms in the presence of low NO_x and VOC levels. The heightened sensitivity to VOC levels does support the argument that the additional ketone chemistry in the CB6R3 model is an important pathway for O_3 production.

Winter

Interpretation of the winter O_3 formation is a little more complicated. Both O_3 and NO_x levels are elevated regionally (Figure 3), while NO_x emissions are reduced, and VOC emissions remain the same (Figure 2). The elevated NO_x levels could be due to a lower PBL that is not well-compensated by the KZMIN factor used in the model. This is consistent with the poorer NMB metrics at all sites in the study area (Figure 6) and the general under-prediction seen in the O_3 winter time series (Figure 4). Sorting out the impact of different chemical mechanisms in the winter must allow not only for the variation in PBL but also for the complication of the atmosphere receiving significantly less actinic flux at these latitudes. When the CB6R3 case was compared to the other two mechanisms, the variation in the entire domain was between -0.75% – 0% (Figure 5e,f), except near the Grande Prairie area, where the O_3 production difference with SAPRC07 was slightly higher (Figure 5e). While the O_3 formation was, in general, poorer in the winter, the slight enhancement in CB6R3 performance implies that the differences in the mechanisms are more evident in the winter in the high NO_x and high VOCs areas.

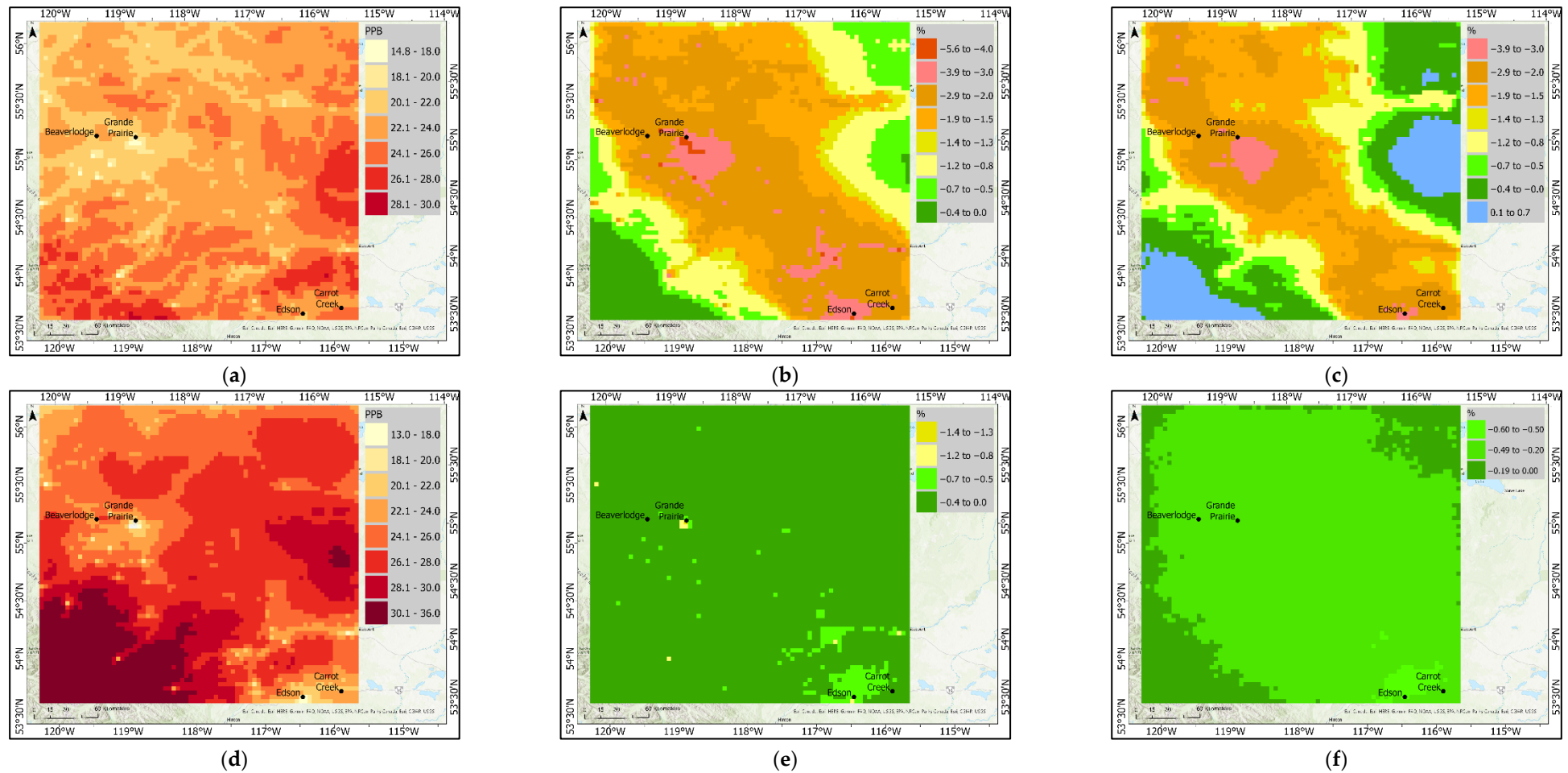


Figure 5. (a) Predicted average hourly O₃ concentrations for (a) CB6R3 (summer), (b) CB6R3 vs. SAPRC07¹ (summer), (c) CB6R3 vs. RACM2² (summer), (d) CB6R3 (winter), (e) CB6R3 vs. SAPRC07¹ (winter), (f) CB6R3 vs. RACM2² (winter). ¹ $[100 * (\text{SAPRC07} - \text{CB6R3} / \text{CB6R3})]$ ² $[100 * (\text{RACM2} - \text{CB6R3} / \text{CB6R3})]$.

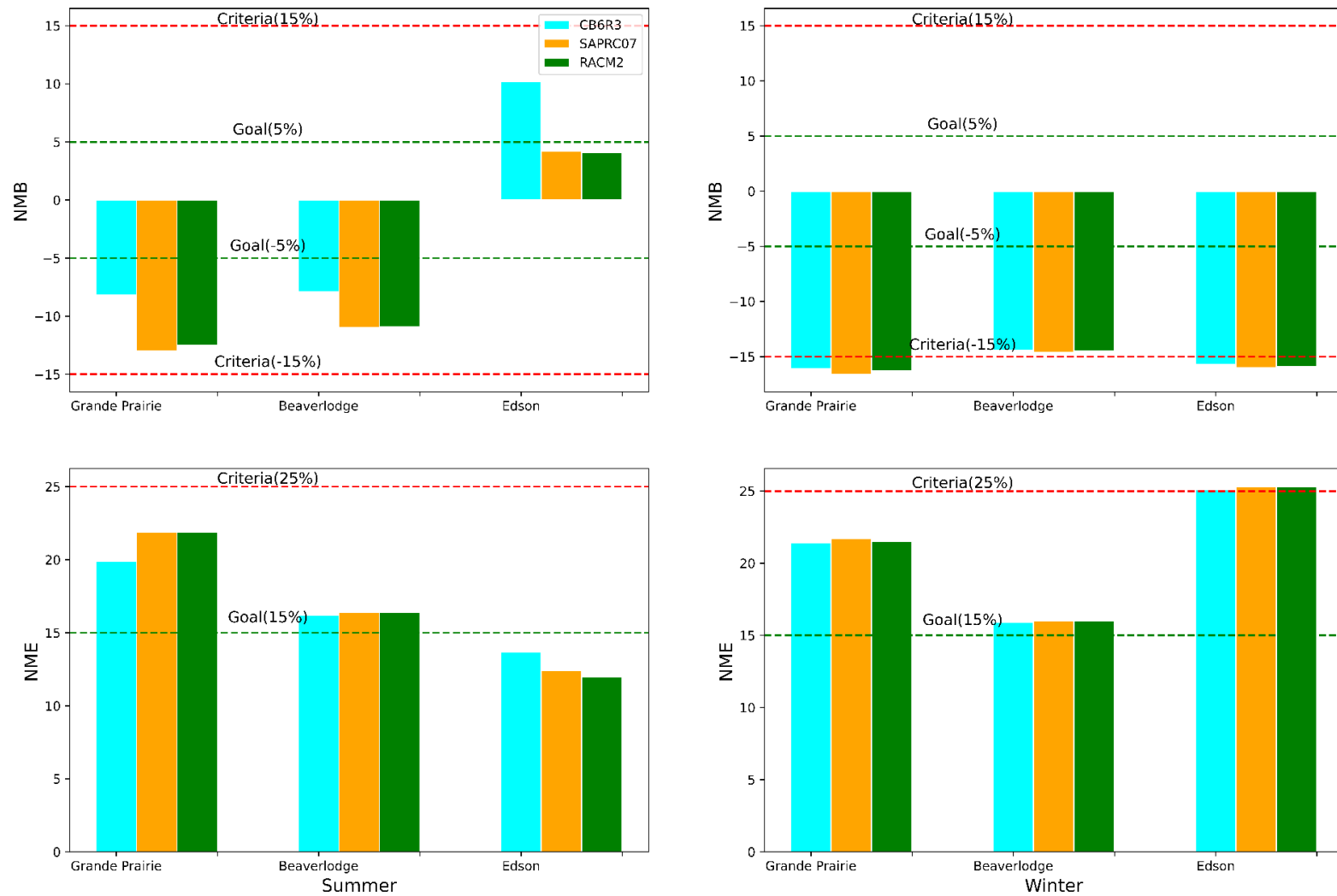


Figure 6. O₃ model performance, as measured by NMB and NME, at three ambient monitoring stations in summer (left) and winter (right).

3.2.3. Model Performance

Figure 6 shows NMB and NME results for average hourly O₃ concentration during the summer and winter months at the Grande Prairie, Beaverlodge, and Edson stations.

Grande Prairie

In summer, all three mechanisms meet the NMB and NME criteria, while none meet the goal. CB6R3 performed better followed by RACM2 and SAPRC07. In winter, the NMB criteria were exceeded, and the NME criteria were met by all three mechanisms. As was the case for the summer, CB6R3 performed slightly better for all criteria than the other mechanisms. The modest improvement in the performance of CB6R3 relative to the other mechanisms may be attributed to additional organic pathways to produce O₃.

Beaverlodge

O₃ predictions by all three mechanisms followed a similar pattern as Grande Prairie, with all mechanisms performing slightly better at this station. NMB and NME criteria were met in both seasons. Summer NMB values were better than winter, while NME values were similar in both seasons. Beaverlodge is a low NO_x and moderately high VOC area, as depicted in the emissions heat map (Figure 2). CB6R3 appears to show better performance compared to the other mechanisms under these conditions.

Edson

During summer, both RACM2 and SAPRC07 meet the NMB goal but the CB6R3 NMB is considerably higher, so it does not meet the goal but does meet the criteria. In winter, all three mechanisms exceed the NME criteria. Edson is a both a moderately high NO_x and VOC emission area, but the KZMIN value in winter at this site, as for the other sites, may not be appropriate and may be significantly biasing the models to be low. Under these conditions, CB6R3 seems to provide a very marginal improvement in performance.

3.2.4. Discussion

Predictions of O₃ will be affected by the choice of mechanism as well as KZMIN. For each site, the variation in the statistics of the three mechanisms is significantly greater in the summer, with CB6R3 performing better at two of the three sites (Grand Prairie, Beaverlodge) during the summer and marginally better at all sites during the winter. This does suggest that the additional chemical pathways for forming O₃ contained in the CB6R3 model are an improvement. However, this improvement is not universal, with Edson being better modelled with SAPRC07 and RACM2 during the summer. It is possible that Edson is being influenced by such factors as the composition of its emissions and/or meteorology. Grand Prairie and Beaverlodge are relatively close together, so these sites may be impacted by similar sources under similar meteorological conditions.

Another possible explanation for the variation in performance between the mechanisms may be the appropriate choice of KZMIN. Grand Prairie is a larger population centre and is well-characterized as urban, so the choice of KZMIN should be clear. Beaverlodge is a very small population centre and should be well-characterized as rural. Edson is also a relatively small population centre, but it may be mischaracterized as an urban centre, when a rural designation may be more appropriate. Additional sensitivity studies will be required to clearly delineate the impact of the choice of KZMIN.

3.3. Fine Particulate (PM_{2.5})

Fine particulate (PM_{2.5}) is defined as the sum of the following species [10], where each species is the sum of the Aitken (i) and accumulation modes (j) of their respective aerosols:

$$PM_{2.5} = ASO4 + ANO3 + ANH4 + AEC + ANA + ACL + AXYL1 + AXYL2 + AXYL3 + ATOL1 + ATOL2 + ATOL3 + ABNZ1 + ABNZ2 + ABNZ3 + AISO1 + AISO2 + AISO3 + ATRP1 + ATRP2 + ASQT + AOLGA + AOLGB + AORGC$$

The description of each species is provided in Table S2.

3.3.1. Spatial Variation

The spatial distribution of primary $PM_{2.5}$ emission by season is presented in Figure 2. Non-point sources are the largest source of primary $PM_{2.5}$ (Table 2), so there is no surprise that there is a strong spatial correlation of this component of $PM_{2.5}$ with roadways as well as with urban centres—Grande Prairie, Beaverlodge, and Edson. The spatial variation of average $PM_{2.5}$ predicted by CB6R3 in summer and winter, as well as the respective differences with SAPRC07 and RACM2, are shown in Figure 7. During the summer, low concentrations are observed in the south and southwest of the domain, with slightly higher concentrations to the north and east. There is a strong spatial correlation during the summer months between these slightly higher concentrations and roadways. During the winter, the primary $PM_{2.5}$ is elevated throughout the modelling domain (Figure 2), with noticeable enhancements around the urban centres. The spatial pattern for winter now runs from northwest to southeast, aligning more with the NO_x and VOC emissions. Generally, the winter concentrations were higher than the summer concentrations. In summer, SAPRC07 and RACM2 produced up to 11% and 14% more $PM_{2.5}$ than CB6R3, respectively. In winter, CB6R3 and SAPRC07 were similar, but RACM2 produced up to 7% more than CB6R3.

The change in spatial correlation between winter and summer may suggest a change in the source of the $PM_{2.5}$. Figure 8 shows mean concentrations in the study area for various species of $PM_{2.5}$ such as nitrate (ANO_3), sulfate (ASO_4), ammonium (ANH_4), and Secondary Organic Aerosols (SOA) for anthropogenic and biogenic sources produced by CB6R3, SAPRC07, and RACM2 mechanisms. Clearly there is a difference in $PM_{2.5}$ composition between summer and winter.

Figure 9 depicts the relative percentage composition of nitrate, sulfate, ammonium, SOA-Anthropogenic (SOA-Anth), and SOA Biogenic (SOA-Bio) predicted by three mechanisms for both summer and winter. Sulfate and SOA-Bio dominates $PM_{2.5}$ in summer and were approximately 50% and 35%, respectively, of the total. Nitrate production during the summer was very low for all mechanisms. Other species combined were about 15%, but SAPRC07 produced about 10% more SOA-Bio and 7% more SOA-Anth. There is a noticeable difference in the production of nitrate compounds during winter. CB6R3 produced the most sulfate, followed by SAPRC07 and RACM2. In the winter, the most dominant $PM_{2.5}$ species were nitrate (64%), sulfate (21%), and ammonium (10%). Other species were at less than 10%. The three mechanisms showed no major difference in terms of relative compositions in the winter.

3.3.2. Model Performance

To evaluate $PM_{2.5}$ modelling performance for each chemical mechanism, various statistical performance benchmarks were used. Figure 10 shows NMB, NME, FB, and FE at three monitoring sites during summer and winter.

Grande Prairie

The model exhibits an underestimation bias in both summer and winter. In the summer, none of the chemical mechanisms meet the NMB, NME, FB, or FE criteria, though RACM2 performed slightly better than both SAPRC07 and CB6R3 in terms of lower bias and error. At the Grande Prairie site, all mechanisms operate better in the winter, and the RACM2 mechanism outperforms the other two chemical mechanisms.

Beaverlodge

At Beaverlodge as well, the model exhibits underestimation bias, like Grande Prairie. All three mechanisms miss the NMB, NME, FB, and FE goals and criteria and have similar performance, though RACM2 appears to outperform the other mechanisms slightly in both bias and error. The three mechanisms perform similarly during summer and winter.

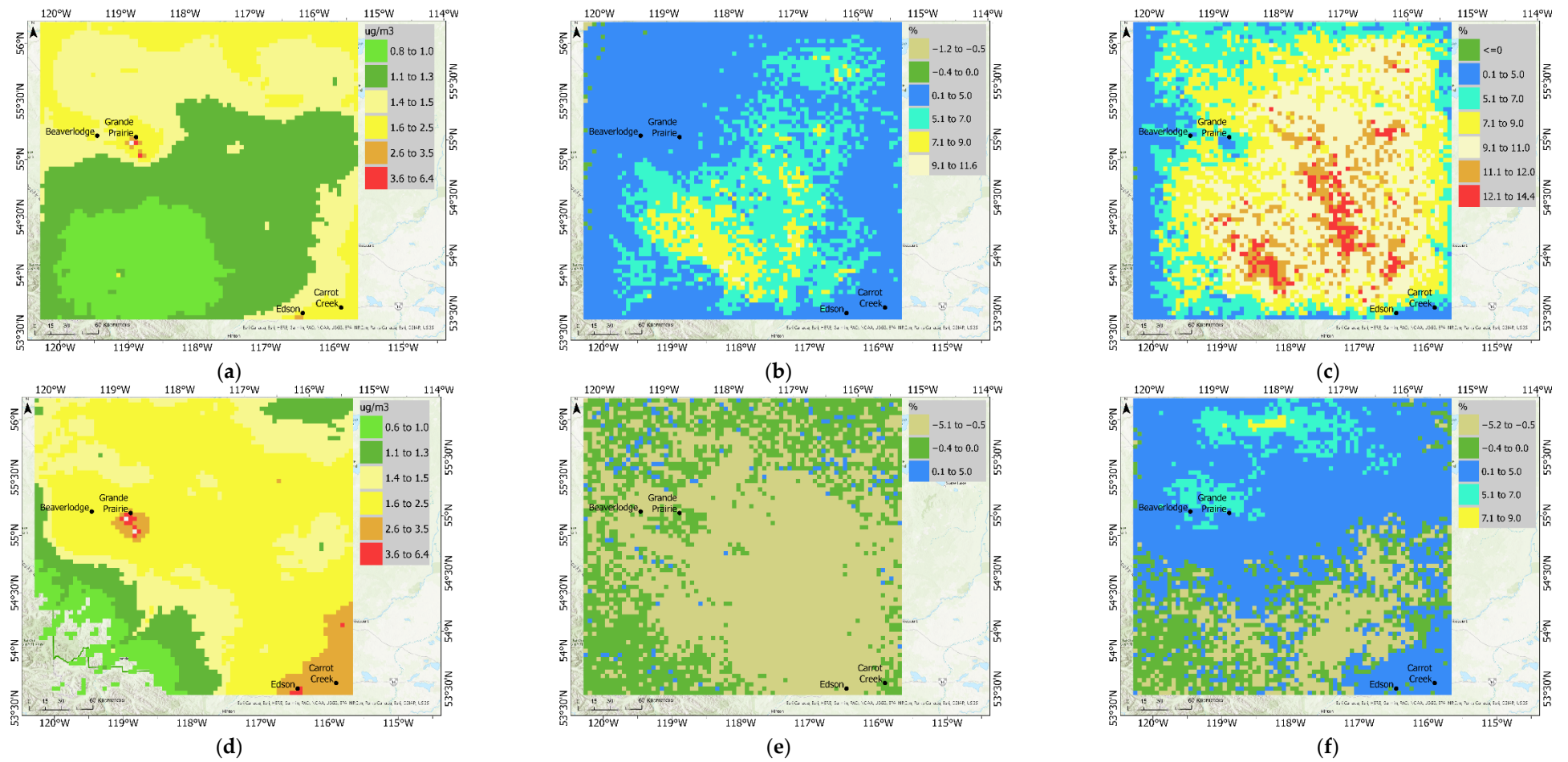


Figure 7. (a) Predicted average hourly PM_{2.5} concentrations for (a) CB6R3 (summer), (b) CB6R3 vs. SAPRC07¹ (summer), (c) CB6R3 vs. RACM2 2 (summer), (d) CB6R3 (winter), (e) CB6R3 vs. SAPRC07¹ (winter), (f) CB6R3 vs. RACM2 2 (winter). ¹ $[100 \cdot (\text{SAPRC07} - \text{CB6R3}) / \text{CB6R3}]$ ² $[100 \cdot (\text{RACM2} - \text{CB6R3}) / \text{CB6R3}]$.

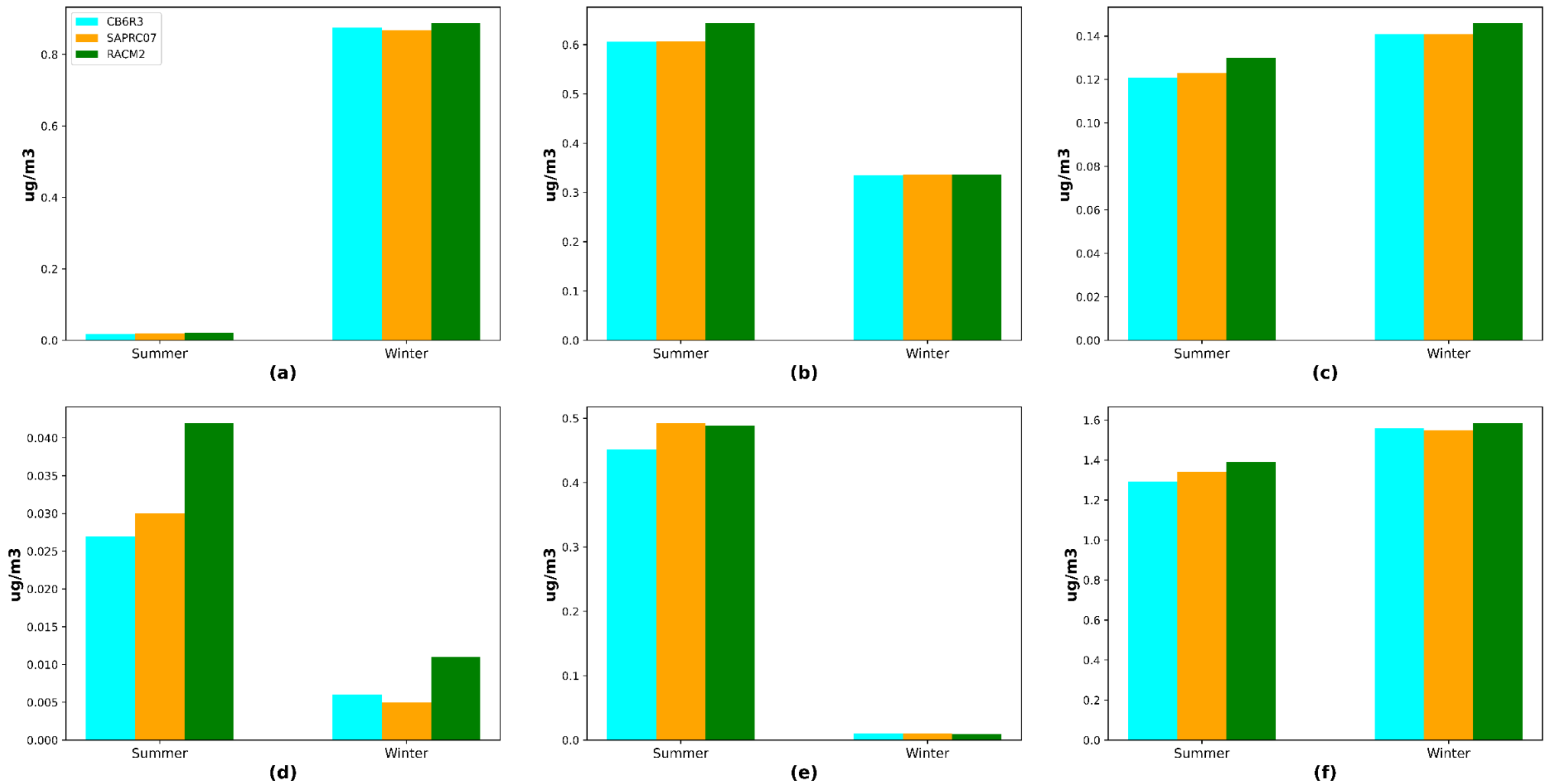


Figure 8. Comparison of CB6R3, SAPRC07, and RACM2 predicted monthly mean values for (a) Nitrate, (b) Sulphate (c) Ammonium, (d) SOA-Antropogenic, (e) SOA-Biogenic, (f) Total fine particulate ($\text{PM}_{2.5}$).

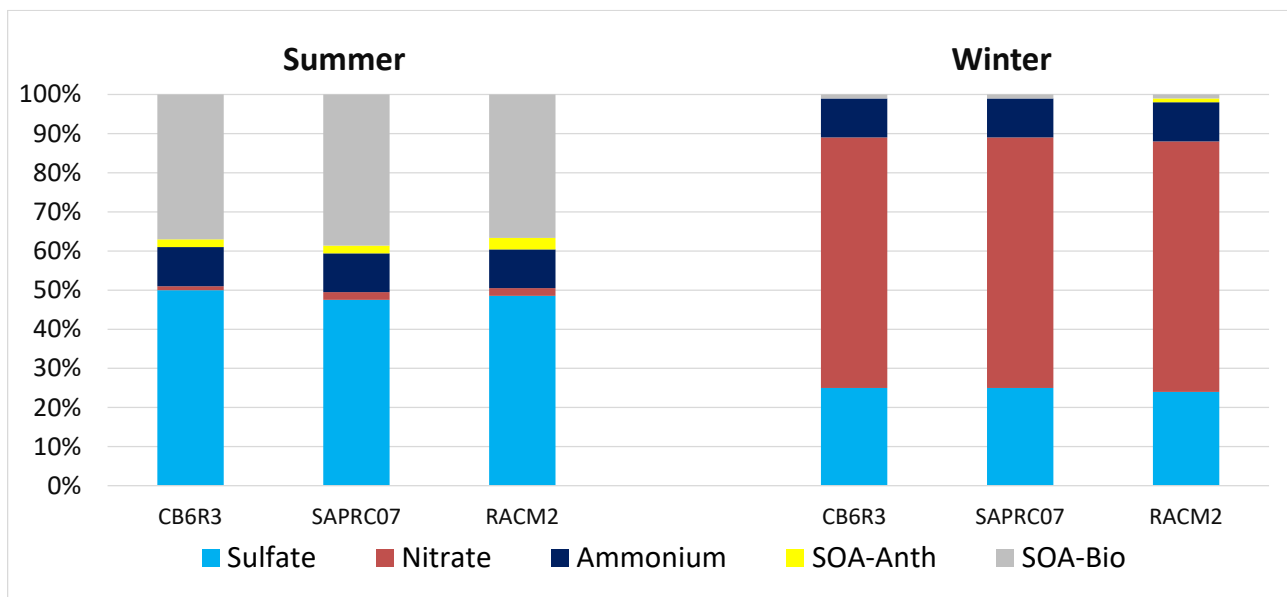


Figure 9. Percentage relative compositions of key species for PM_{2.5} predicted during summer (left) and winter (right).

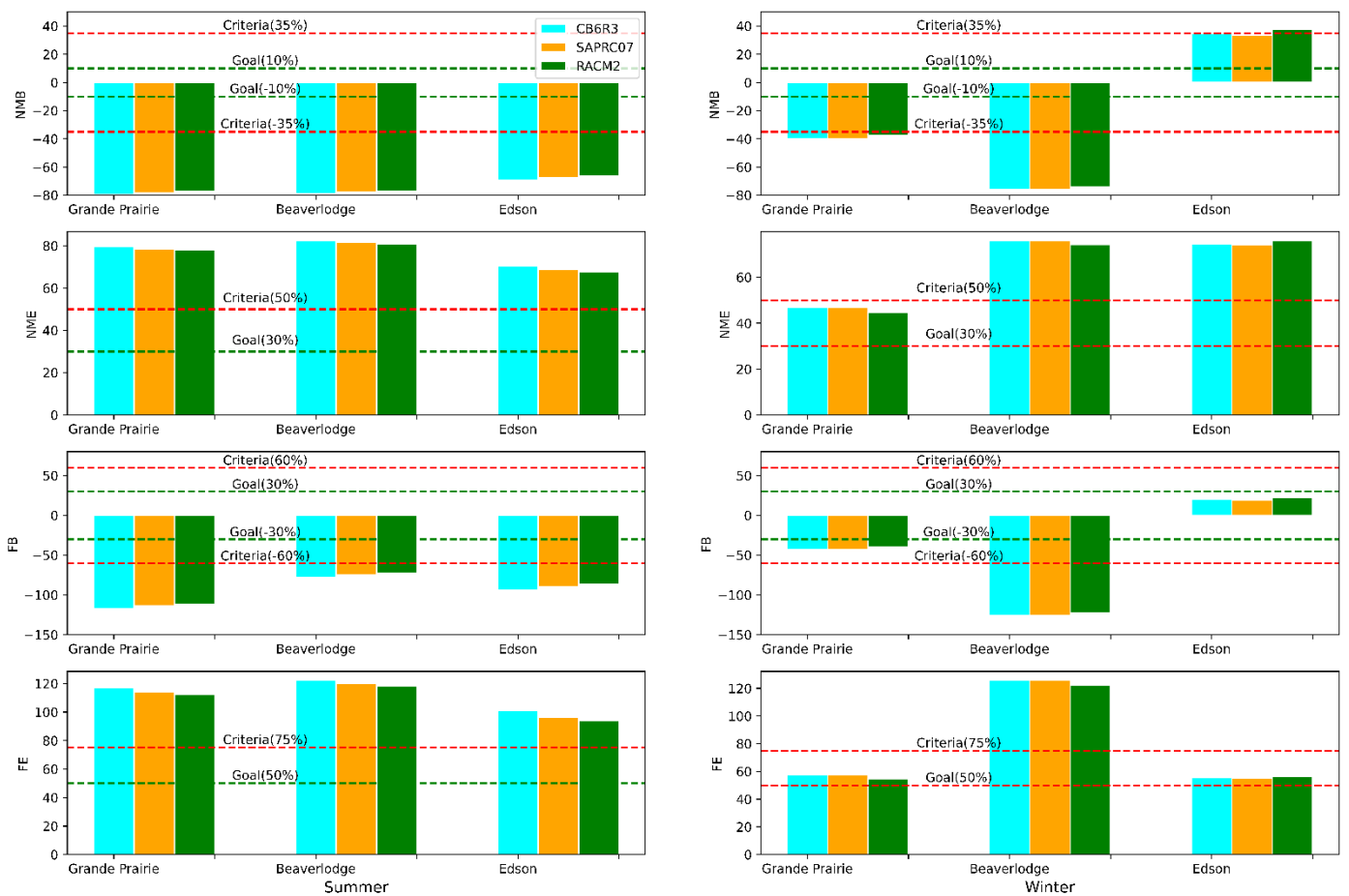


Figure 10. PM_{2.5} model performance as measured by NMB, NME, FB, and FE at three ambient monitoring stations in summer (left) and winter (right).

Edson

In the summer, all three mechanisms missed the NMB, NME, and FB criteria, but met the FE criteria. Winter performance is better. The NMB and NME criteria are met by all three mechanisms, with SAPRC07 outperforming the other mechanisms slightly. All three mechanisms meet the FB and FE goal, and again SAPRC07 performed the best, followed by RACM2 and CB6R3.

3.3.3. Discussion

All three mechanisms under-predicted PM_{2.5} concentrations. Of the three, RACM2 performed slightly better, except at Edson where it was slightly worse. The Secondary Organic Aerosol Model (SORGAM) used in this study was originally developed on the basis of the absorption properties of organic aerosol, to better model the formation of low-volatility products from reactive organic gases via oxidation by OH, NO₃, or O₃, as well as their subsequent gas/particle partitioning [52]. This method was then extended to include the available species in the RACM chemistry, by creating eight classes representing anthropogenic (four—two aromatic, one higher alkane, one higher alkene) and biogenic (four—two for α -pinene, two for limonene) gas/particle equilibria [52]. Of particular note was the complexity of describing the non-linear relationship between the primary and secondary aerosols, as well as the strong dependence on temperature for driving the equilibria, i.e., lower temperatures favored particle formation.

The present study employed more up-to-date chemical mechanisms with improved reaction rates, rate constants, and products. As an example, RACM2 has been updated to incorporate better chemistry for aromatics, isoprene, alcohols (in remote areas), and acetone (in the upper atmosphere) [12]. The enhanced production of SOA-Anth and sulfate (Figure 8) by RACM2, over the other mechanisms for all seasons, suggests both the organic and inorganic anthropogenic particulate is best modelled by this mechanism. SOA-Bio and NH₄ production is similar between the mechanisms, with SAPRC07 slightly better at producing SOA-Bio, though this difference is probably not significant.

The most striking change in the PM_{2.5} formation is the change from being a SO₄/SAO-Bio-dominated region in the summer to a NO₃-dominated region in the winter (Figure 9). Clearly the PM_{2.5} chemistry has changed during these periods. Pathak et al. [53] noted the sensitivity of SOA formation on the ratio of the molar concentration of NH₄ to SO₄, with SO₄ being preferentially formed in NH₄-poor regions, i.e., where [NH₄]/[SO₄] molar <1.5. Song et al. [54], in a similar study in NH₄-rich agricultural region, noted the molar ratio of NO₃ to SO₄ would indicate whether the SOA was being produced by mobile sources or non-mobile sources, with a low ratio being characteristic of non-mobile emissions and a high ratio being characteristic of mobile emissions (13:1—gasoline; 8:1 diesel). Table 4 presents a summary of relevant information from this study for comparison.

Table 4. Summary of NO₃, SO₄, and NH₄ ratios governing SOA formation.

Species	Summer		Winter	
	[$\mu\text{g}/\text{m}^3$]	[$\mu\text{mol}/\text{m}^3$]	[$\mu\text{g}/\text{m}^3$]	[$\mu\text{mol}/\text{m}^3$]
NO ₃	2.00×10^{-2}	3.20×10^{-4}	9.00×10^{-1}	1.45×10^{-2}
SO ₄	6.50×10^{-1}	6.80×10^{-3}	3.30×10^{-1}	3.40×10^{-3}
NH ₄	1.30×10^{-1}	7.20×10^{-3}	1.42×10^{-1}	7.90×10^{-3}
Ratio				
NH ₄ /SO ₄		1.05		2.33
NH ₄ Type		poor		rich
NO ₃ /SO ₄		4.70×10^{-1}		4.27
SOA Source		Non-mobile		Mobile/ some non-mobile

During the summer, the region is NH₄-poor (NH₄/SO₄ < 1.5), which should drive SOA towards high SO₄ content. This is indeed the case (Figure 8). During the winter the

region is relatively NH_4 -rich, and it is colder (which should favor NO_3 formation), which is observed, albeit with an appreciable amount of SO_4 still present. The NO_3 component may be attributable to local mobile sources (preferably diesel over gasoline), while the persistent SO_4 contribution may be a blend of mobile sources and non-mobile sources, such as the oil and gas activity in the area.

Comparing the spatial distribution of $\text{PM}_{2.5}$ for winter and summer (Figure 2) also provides some indication of the nature of SOA production in the region. The summer map shows some correlation between the transportation corridors and $\text{PM}_{2.5}$ but is weaker with NO_x . Many of the roads visible in $\text{PM}_{2.5}$ but not NO_x are probably unpaved or secondary roads with reduced traffic, which are still quite dusty, i.e., high primary $\text{PM}_{2.5}$ emissions. The winter map shows generally elevated $\text{PM}_{2.5}$ throughout the region, probably due to colder temperatures and elevated aerosol NO_3 production, with secondary roads still clearly visible. All the mechanisms agree closely where the primary $\text{PM}_{2.5}$ is dominant (urban centres), but SAPRC07 and RACM2 show some improvement in modelling $\text{PM}_{2.5}$ where there are lower VOC levels.

4. Summary and Conclusions

The three chemical mechanisms (CB6R3, SAPRC07 and RACM2) were implemented in the CMAQ modelling system, and two-month simulations, one in summer and one in winter, were run. The model predictions of various species by each of the mechanisms are compared to one another and to the observed data. Many chemical species concentrations predicted by the three mechanisms differed by relatively large margins. In summer, the simulation with CB6R3 predicted a higher concentration of H_2O_2 and PAN, while RACM2 predicted higher concentrations of OH, NO_x , and O_3 . SAPRC07 produced high concentrations of MEPX. The winter ratios, with respect to difference mechanism, were like summer but predicted significantly lower concentrations except for NO_x and O_3 . The analysis of diurnal variation of O_3 at four stations revealed that SAPRC07 and RACM2 predictions were higher in the early part of the day, while CB6R3 predictions were the highest at noon. In summer, CB6R3 produces higher levels of O_3 in the presence of higher VOCs and NO_x levels, while producing low levels of O_3 in the presence of high NO_x levels; however, in winter, the difference in the production of O_3 due to the three mechanisms was negligible.

An analysis of the spatial and temporal variation of the aerosol components of $\text{PM}_{2.5}$ shows a significant shift from SO_4 -dominated $\text{PM}_{2.5}$ in the summer to NO_3 -dominated $\text{PM}_{2.5}$ in the winter. This shift is probably due to a change in the relative concentration of NH_4 to SO_4 and the temperature. Furthermore, the winter $\text{PM}_{2.5}$ is probably due to mobile emissions, with some SO_4 coming from oil and gas activity in the region, while summer $\text{PM}_{2.5}$ is due to non-mobile emissions related to anthropogenic sources and oil and gas activity in the region. Of the three mechanisms tested, RACM2 seems to be marginally better at capturing this variability.

A statistical comparison of predicted and observed data from various stations revealed that O_3 performance is dependent on chemical mechanisms and the station. In summer, RACM2 and SAPRC07 performed better at Edson, while CB6R3 was better at the other two stations. No mechanism accurately captures wintertime O_3 . When compared to other mechanisms, $\text{PM}_{2.5}$ predictions with RACM2 were slightly better. The dominant $\text{PM}_{2.5}$ species in summer were SO_4 and SOA-Bio, while NO_3 and SO_4 were dominant in winter. The NO_3 species were significantly higher in winter.

The difference in the model predictions of O_3 and $\text{PM}_{2.5}$ by the three chemical mechanisms are sufficiently different, so it may impact the categorization of an area for the suitable CAAQS management zone. Moreover, the appropriate choice of KZMIN will produce variation in O_3 and $\text{PM}_{2.5}$ predictions. When running an air quality model for O_3 control strategies, CB6R3 performs slightly better at the urban stations than the other mechanisms, with RACM2 also showing good performance in rural areas. When modelling for $\text{PM}_{2.5}$ control strategies, RACM2 appears to be the better mechanism. More modelling is necessary with O_3 and $\text{PM}_{2.5}$ control scenarios using the three mechanisms, and KZMIN

sensitivity studies will be required for further understanding of the implications on using one mechanism over other.

Supplementary Materials: The following supporting information can be downloaded at: <https://www.mdpi.com/article/10.3390/app12178576/s1>, Figure S1: Historical Annual Average NO₂; Figure S2: Historical 3-year Average 4th Highest Daily max 8-h O₃; Figure S3: Historical Daily Average PM_{2.5}; Table S1: CAAQS Management Levels; Table S2: Model Species and their Descriptions.

Author Contributions: Conceptualization, M.S. and M.Z.; Data curation, S.C.; Formal analysis, M.S. and M.Z.; Methodology, M.S.; Project administration, S.H.; Resources, S.H.; Validation, S.C., D.L., M.Z. and S.H.; Writing—original draft, M.S.; Writing—review & editing, S.C., D.L. and S.H. All authors have read and agreed to the published version of the manuscript.

Funding: This research received no external funding.

Acknowledgments: We gratefully acknowledge Alberta Energy Regulator for providing resources to run the air quality model and Alberta Environment and Parks for providing meteorological and emissions data.

Conflicts of Interest: The authors declare no conflict of interest.

References

1. Lefohn, A.S.; Malley, C.S.; Smith, L.; Wells, B.; Hazucha, M.; Simon, H.; Naik, V.; Mills, G.; Schultz, M.G.; Paoletti, E.; et al. Tropospheric ozone assessment report: Global ozone metrics for climate change, human health, and crop/ecosystem research. *Elem. Sci. Anthr.* **2018**, *6*, 7. [CrossRef] [PubMed]
2. Wilson, S.R.; Madronich, S.; Longstreth, J.D.; Solomon, K.R. Interactive effects of changing stratospheric ozone and climate on tropospheric composition and air quality, and the consequences for human and ecosystem health. *Photochem. Photobiol. Sci.* **2019**, *18*, 775–803. [CrossRef] [PubMed]
3. Grulke, N.E.; Heath, R.L. Ozone effects on plants in natural ecosystems. *Plant Biol.* **2019**, *22*, 12–37. [CrossRef] [PubMed]
4. Xu, X.; Lin, W.; Xu, W.; Jin, J.; Wang, Y.; Zhang, G.; Zhang, X.; Ma, Z.; Dong, Y.; Ma, Q.; et al. Long-term changes of regional ozone in China: Implications for human health and ecosystem impacts. *Elem. Sci. Anthr.* **2020**, *8*, 13. [CrossRef]
5. Stieb, D.M.; Evans, G.J.; To, T.M.; Brook, J.R.; Burnett, R.T. An ecological analysis of long-term exposure to PM_{2.5} and incidence of COVID-19 in Canadian health regions. *Environ. Res.* **2020**, *191*, 110052. [CrossRef]
6. Domingo, J.L.; Rovira, J. Effects of air pollutants on the transmission and severity of respiratory viral infections. *Environ. Res.* **2020**, *187*, 109650. [CrossRef]
7. ApSimon, H.; Oxley, T.; Woodward, H.; Mehlig, D.; Dore, A.; Holland, M. The UK Integrated Assessment Model for source apportionment and air pollution policy applications to PM_{2.5}. *Environ. Int.* **2021**, *153*, 106515. [CrossRef]
8. Oikonomakis, E.; Aksoyoglu, S.; Ciarelli, G.; Baltensperger, G.; Prévôt, A.S.H. Low modeled ozone production suggests underestimation of precursor emissions (especially NO_x) in Europe. *Atmos. Chem. Phys.* **2018**, *18*, 2175–2198. [CrossRef]
9. Shareef, M.; Husain, T.; Alharbi, B. Studying the Effect of Different Gas-Phase Chemical Kinetic Mechanisms on the Formation of Oxidants, Nitrogen Compounds and Ozone in Arid Regions. *J. Environ. Prot.* **2019**, *10*, 1006–1031. [CrossRef]
10. Nopmongcol, U.; Johnson, J.; Shah, T.; Vennam, P.; Trail, M.; Morris, R.; Allan, W.; Qiu, X.; Vatcher, C.; Yang, F. *Provincial Air Quality Photochemical Modelling Final Report*; Prepared for Alberta Environment and Parks; Ramboll: Novata, CA, USA; Novus Environmental: Guelph, ON, Canada, 2018.
11. Li, X.; Rappenglueck, B. A study of model nighttime ozone bias in air quality modeling. *Atmos. Environ.* **2018**, *195*, 210–228. [CrossRef]
12. Goliff, W.S.; Stockwell, W.R.; Lawson, C.V. The regional atmospheric chemistry mechanism, version 2. *Atmos. Environ.* **2013**, *68*, 174–185. [CrossRef]
13. Carter, W.P. Development of the SAPRC-07 chemical mechanism. *Atmos. Environ.* **2010**, *44*, 5324–5335. [CrossRef]
14. Gery, M.W.; Whitten, G.Z.; Killus, J.P.; Dodge, M.C. A photochemical kinetics mechanism for urban and regional scale computer modeling. *J. Geophys. Res. Atmos.* **1989**, *94*, 12925–12956. [CrossRef]
15. Yarwood, G.; Rao, S.; Yocke, M.; Whitten, G. Updates to the Carbon Bond Chemical Mechanism: CB05. Final report to the US EPA, RT-0400675. 2005. Available online: [http://www.camx.com/publ/pdfs/cb05final%\\$backslash\\$report%\\$backslash\\$120805.aspx](http://www.camx.com/publ/pdfs/cb05final%$backslash$report%$backslash$120805.aspx) (accessed on 1 July 2015).
16. Whitten, G.Z.; Heo, G.; Kimura, Y.; McDonald-Buller, E.; Allen, D.T.; Carter, W.P.; Yarwood, G. A new condensed toluene mechanism for Carbon Bond: CB05-TU. *Atmos. Environ.* **2010**, *44*, 5346–5355. [CrossRef]
17. Stockwell, W.R. A homogeneous gas phase mechanism for use in a regional acid deposition model. *Atmos. Environ.* **1986**, *20*, 1615–1632. [CrossRef]
18. Stockwell, W.R.; Middleton, P.; Chang, J.S.; Tang, X. The second-generation regional acid deposition model chemical mechanism for regional air quality modeling. *J. Geophys. Res. Atmos.* **1990**, *95*, 16343–16367. [CrossRef]

19. Stockwell, W.R.; Kirchner, F.; Kuhn, M.; Seefeld, S. A new mechanism for regional atmospheric chemistry modeling. *J. Geophys. Res.* **1997**, *102*, 25847–25879. [[CrossRef](#)]
20. RACM2 Species: USAEPA CMAQ. Available online: https://github.com/USEPA/CMAQ/blob/main/CCTM/src/MECHS/mechanism_information/racm2_ae6_aq/racm2_ae6_aq_species_table.md (accessed on 16 August 2022).
21. SAPRC07 Species: USAEPA CMAQ. Available online: https://github.com/USEPA/CMAQ/blob/main/CCTM/src/MECHS/mechanism_information/saprc07tc_ae6_aq/saprc07tc_ae6_aq_species_table.md (accessed on 16 August 2022).
22. Carter, W.P. Documentation of the SAPRC-99 chemical mechanism for VOC reactivity assessment. *Contract* **2000**, *92*, 95–308.
23. Sarwar, G.; Luecken, D.; Yarwood, G.; Whitten, G.Z.; Carter, W.P. Impact of an updated carbon bond mechanism on predictions from the CMAQ modeling system: Preliminary assessment. *J. Appl. Meteorol. Climatol.* **2008**, *47*, 3–14. [[CrossRef](#)]
24. CB6R3 Species: USAEPA CMAQ. Available online: https://github.com/USEPA/CMAQ/blob/main/CCTM/src/MECHS/mechanism_information/cb6r3_ae7_aq/cb6r3_ae7_aq_species_table.md (accessed on 16 August 2022).
25. Emery, C.; Jung, J.; Downey, N.; Johnson, J.; Jimnez, M.; Yarwood, G.; Morris, R. Regional and global modeling estimates of policy relevant background ozone over the United States. *Atmos. Environ.* **2012**, *47*, 206–217. [[CrossRef](#)]
26. Luecken, D.J.; Yarwood, G.; Hutzell, W.T. Multipollutant modeling of ozone, reactive nitrogen and HAPs across the continental US with CMAQ-CB6. *Atmos. Environ.* **2019**, *201*, 62–72. [[CrossRef](#)] [[PubMed](#)]
27. Jimenez, P.; Baldasano, J.M.; Dabdub, D. Comparison of photochemical mechanisms for air quality modeling. *Atmos. Environ.* **2003**, *37*, 4179–4194. [[CrossRef](#)]
28. Gross, A.; Stockwell, W.R. Comparison of the EMEP, RADM2 and RACM mechanisms. *J. Atmos. Chem.* **2003**, *44*, 151–170. [[CrossRef](#)]
29. Byun, D.; Schere, K.L. Review of the governing equations, computational algorithms, and other components of the Models-3 Community Multiscale Air Quality (CMAQ) modeling system. *Appl. Mech. Rev.* **2006**, *59*, 51–77. [[CrossRef](#)]
30. Faraji, M.; Kimura, Y.; McDonald-Buller, E.; Allen, D. Comparison of the carbon bond and SAPRC photochemical mechanisms under conditions relevant to southeast Texas. *Atmos. Environ.* **2008**, *42*, 5821–5836. [[CrossRef](#)]
31. Luecken, D.J.; Phillips, S.; Sarwar, G.; Jang, C. Effects of using the CB05 vs. SAPRC99 vs. CB4 chemical mechanism on model predictions: Ozone and gas-phase photochemical precursor concentrations. *Atmos. Environ.* **2008**, *42*, 5805–5820. [[CrossRef](#)]
32. Sarwar, G.; Godowitch, J.; Henderson, B.H.; Fahey, K.; Pouliot, G.; Hutzell, W.T.; Mathur, R.; Kang, D.; Goliff, W.S.; Stockwell, W.R. A comparison of atmospheric composition using the Carbon Bond and Regional Atmospheric Chemistry Mechanisms. *Atmos. Chem. Phys.* **2013**, *13*, 9695–9712. [[CrossRef](#)]
33. Gupta, M.; Mohan, M. Validation of WRF/Chem model and sensitivity of chemical mechanisms to ozone simulation over megacity Delhi. *Atmos. Environ.* **2015**, *122*, 220–229. [[CrossRef](#)]
34. Kitayama, K.; Morino, Y.; Yamaji, K.; Chatania, S. Uncertainties in O₃ concentrations simulated by CMAQ over Japan using four chemical mechanisms. *Atmos. Environ.* **2019**, *198*, 448–462. [[CrossRef](#)]
35. Chen, C.H.; Chen, T.F.; Huang, S.P.; Chang, K.H. Comparison of the RADM2 and RACM chemical mechanisms in O₃ simulations: Effect of the photolysis rate constant. *Sci. Rep.* **2021**, *11*, 1–15. [[CrossRef](#)]
36. Cao, L.; Li, S.; Sun, L. Study of different Carbon Bond 6 (CB6) mechanisms by using a concentration sensitivity analysis. *Atmos. Chem. Phys.* **2021**, *21*, 12687–12714. [[CrossRef](#)]
37. Municipal District of Greenview Data, Government of Alberta. Available online: <https://regionaldashboard.alberta.ca/region/greenview-no-16/#/> (accessed on 16 August 2022).
38. Canadian Council of Ministers of the Environment. Guidance Document on Air Zone Management. 2019. Available online: https://ccme.ca/en/res/guidancedocumentonairzonemanagement_secured.pdf (accessed on 14 August 2022).
39. Skamarock, W.C.; Klemp, J.B.; Dudhia, J.; Gill, D.O.; Barker, D.M.; Wang, W.; Powers, J.G. A description of the Advanced Research WRF version 3. NCAR Technical note 475. 2008.
40. NPRI 2013 (National Pollutant Release Inventory). NPRI Pollutant Inventory. Available online: https://data-donnees.ec.gc.ca/data/substances/plansreports/reporting-facilities-pollutant-release-and-transfer-data/bulk-data-files-for-all-years-releases-disposals-transfers-and-facility-locations/NPRI-INRP_GeolocationsGeolocalisation_1993-present.csv (accessed on 7 August 2022).
41. AEP (Alberta Environment and Parks). *Development of Air Emission Inventories and Modelling Input Files for Upper Athabasca and Upper Peace Regional Strategic Assessment Report*; Alberta Environment and Parks: Edmonton, AB, Canada, 2016.
42. AEP (Alberta Environment and Parks). *Updating Small Upstream Oil and Gas (SUOG) Information of Provincial Air Emissions Inventories in Support of Regional Air Emissions Modelling Report*; Alberta Environment and Parks: Edmonton, AB, Canada, 2017.
43. *Leaf Area Index, Biospheric Atmospheric Interactions Group*; University of California: Irvine, CA, USA, 2019; Available online: <https://bai.ess.uci.edu/megan/data-and-code/lai> (accessed on 16 August 2022).
44. Emery, C.; Liu, Z.; Russell, A.G.; Odman, M.T.; Yarwood, G.; Kumar, N. Recommendations on statistics and benchmarks to assess photochemical model performance. *J. Air Waste Manag. Assoc.* **2017**, *67*, 582–598. [[CrossRef](#)] [[PubMed](#)]
45. Boylan, J.W.; Russell, A.G. PM and Light Extinction Model Performance Metrics, goals and Criteria for Three-Dimensional Air Quality Models. *Atmos. Environ.* **2006**, *40*, 4946–4959. [[CrossRef](#)]
46. Seinfeld, J.H.; Pandis, S.N. *Atmospheric Chemistry and Physics: From Air Pollution to Climate Change*; John Wiley and Sons: Hoboken, NJ, USA, 2012.

47. LaFranchi, B.W.; Wolfe, G.M.; Thornton, J.A.; Harrold, S.A.; Browne, E.C.; Min, K.E.; Woolridge, P.J.; Gilman, J.B.; Kuster, W.C.; Goldan, P.D.; et al. Closing the peroxy acetyl nitrate budget: Observations of acyl peroxy nitrates (PAN, PPN, and MPAN) during BEARPEX 2007. *Atmos. Chem. Phys.* **2009**, *9*, 7623–7641. [[CrossRef](#)]
48. Stockwell, W.R. *Peer Review of the SAPRC-07 Chemical Mechanism Model of Dr. William Carter, Prepared for California Air Resources Board*; Department of Chemistry, Howard University: Washington, DC, USA, 2009.
49. Yarwood, G.; Jung, J.; Whitten, G.Z.; Heo, G.; Mellberg, J.; Estes, E. Updates to the Carbon Bond Mechanism for Version 6 (CB6). In Proceedings of the 9th Annual CMAS Conference, Chapel Hill, NC, USA, 11–13 October 2010.
50. Petetin, H.; Sciare, J.; Bressi, M.; Gros, V.; Rosso, A.; Sanchez, O.; Sarda-Estève, R.; Petit, J.-E.; Beekmann, M. Assessing the ammonium nitrate formation regime in the Paris megacity and its representation in the CHIMERE model. *Atmos. Chem. Phys.* **2016**, *16*, 10419–10440. [[CrossRef](#)]
51. Coates, J.; Mar, K.A.; Ojha, N.; Butler, T.M. The influence of temperature on ozone production under varying NO_x conditions—A modelling study. *Atmos. Chem. Phys.* **2016**, *16*, 11601–11615. [[CrossRef](#)]
52. Schell, B.; Ackermann, I.J.; Hass, H.; Binkowski, F.S.; Ebel, A. Modeling the formation of secondary organic aerosol within a comprehensive air quality model system. *J. Geophys. Res.* **2001**, *106*, 28275–28293. [[CrossRef](#)]
53. Pathak, R.K.; Wu, W.S.; Wang, T. Summertime PM_{2.5} ionic species in four major cities in China: Nitrate formation in an ammonia-deficient atmosphere. *Atos. Chem. Phys.* **2009**, *9*, 1711–1722. [[CrossRef](#)]
54. Song, M.; Kim, M.; Oh, S.-H.; Park, C.; Kim, M.; Kim, M.; Lee, H.; Choe, S.; Bae, M.-S. Influences of Organic Volatile Compounds on the Secondary Organic Carbon of Fine Particulate Matter in the Fruit Tree Area. *Appl. Sci.* **2021**, *11*, 8193. [[CrossRef](#)]